Carbohydrate Polymers 183 (2018) 81–90

Contents lists available at ScienceDirect

Carbohydrate Polymers

journal homepage: www.elsevier.com/locate/carbpol

Research Paper

Sequencing the oligosaccharide pool in the low molecular weight heparin dalteparin with offline HPLC and ESI–MS/MS

Zhangjie Wang[a], Tianji Zhang[b], Shaoshuai Xie[a], Xinyue Liu[a,c], Hongmei Li[b], Robert J. Linhardt[c], Lianli Chi[a,*]

[a] National Glycoengineering Research Center, Shandong University, Jinan 250100, China
[b] Division of Chemical Metrology and Analytical Science, National Institute of Metrology, Beijing 100029, China, China
[c] Center for Biotechnology and Interdisciplinary Studies, Rensselaer Polytechnic Institute, Troy, NY, 12180, United States, United States

ARTICLE INFO

Chemical compounds studied in this article;
Heparin (PubChem CID:
Heparin (PubChem CID: 772)
Dalteparin sodium (PubChem CID: 59350241)

Keywords:
LMWHs
Dalteparin
Sequence
SAX-HPLC
ESI–MS/MS

ABSTRACT

Low molecular weight heparins (LMWHs) are widely used anticoagulant drugs. The composition and sequence of LMWH oligosaccharides determine their safety and efficacy. The short oligosaccharide pool in LMWHs undergoes more depolymerization reactions than the longer chains and is the most sensitive indicator of the manufacturing process. Electrospray ionization tandem mass spectrometry (ESI–MS/MS) has been demonstrated as a powerful tool to sequence synthetic heparin oligosaccharide but never been applied to analyze complicated mixture like LMWHs. We established an offline strong anion exchange (SAX)-high performance liquid chromatography (HPLC) and ESI–MS/MS approach to sequence the short oligosaccharides of dalteparin sodium. With the help of in-house developed MS/MS interpretation software, the sequences of 18 representative species ranging from tetrasaccharide to octasaccharide were obtained. Interestingly, we found a novel 2,3-disulfated hexauronic acid structure and reconfirmed it by complementary heparinase digestion and LC–MS/MS analysis. This approach provides straightforward and in-depth insight to the structure of LMWHs and the reaction mechanism of heparin depolymerization.

1. Introduction

Heparin and low molecular weight heparins (LMWHs) have been widely used as anticoagulant drugs for prevention and treatment of thrombotic diseases due to their high binding affinity to antithrombin III (ATIII), which then inactivates several enzymes of the coagulation system (Gray, Mulloy, & Barrowcliffe, 2008). LMWHs, the depolymerized derivatives of heparin, are more frequently used than their parent heparin because of their more specific bioactivity, reduced bleeding risk, and longer half-life (Hirsh & Levine, 1992). Enoxaparin sodium and dalteparin sodium, the two most important types of LMWHs, are produced by alkaline hydrolysis of heparin benzyl ester and by borohydride reduction after nitrous acid depolymerization, respectively. Both of these LMWHs inherit the backbone structures of parent heparin, the repeating disaccharide of iduronic acid (IdoA) or glucuronic acid (GlcA) residue 1→4 linked to glucosamine (GlcN) residue, with the variable sulfation at 2-*O*-position of hexuronic acid (HexA) residues and the 3-*O*, 6-*O*- and/or *N*-position of the GlcN residues. In addition, the termini of LMWHs are modified by the different depolymerization reactions used in their generation and are distinct from one another. For example, the non-reducing end (NRE) and reducing end (RE) of dalteparin are a 2-*O*-sulfate-α-L-idopyranosyluronic acid residue and a 6-*O*-sulfate-2,5-anhydro-D-mannitol residue (Fig. 1a), while the terminal structures of enoxaparin are an unsaturated uronic acid residue at the NRE and a D-GlcN or 1,6-anhydro structure at the RE in a small percentage (ranging from 15% to 25%) of the enoxaparin chains (Guerrini, Guglieri, Naggi, Sasisekharan, & Torri, 2007).

LMWHs are comprised of linear polyanionic oligosaccharides, and the sequence and composition of these oligosaccharides are essential for their clinical efficacy and safety. Some defined sequences are known to responsible for the anticoagulant activity. For example, a unique pentasaccharide sequence, –GlcNS/Ac6S-GlcA-GlcNS3S6S-IdoA2S-GlcNS6S-, is indispensable for activating ATIII to inhibit coagulation factor Xa (Bisio et al., 2009). A much longer oligosaccharide sequence, containing at least 18 saccharide units and the same pentasaccharide domain, is necessary to inhibit coagulation factor IIa by forming a ternary complex with ATIII together (Chuang, Swanson, Raja, & Olson, 2001). Heparin-induced thrombocytopenia, a major adverse effect of heparin and LMWHs, is closely related to the structure of these drugs (Ahmed, Majeed, & Powell, 2007). Heparin is recognized as one of the

* Corresponding author.
E-mail address: lianlichi@sdu.edu.cn (L. Chi).

https://doi.org/10.1016/j.carbpol.2017.11.039
Received 11 May 2017; Received in revised form 28 October 2017; Accepted 12 November 2017
Available online 13 November 2017
0144-8617/

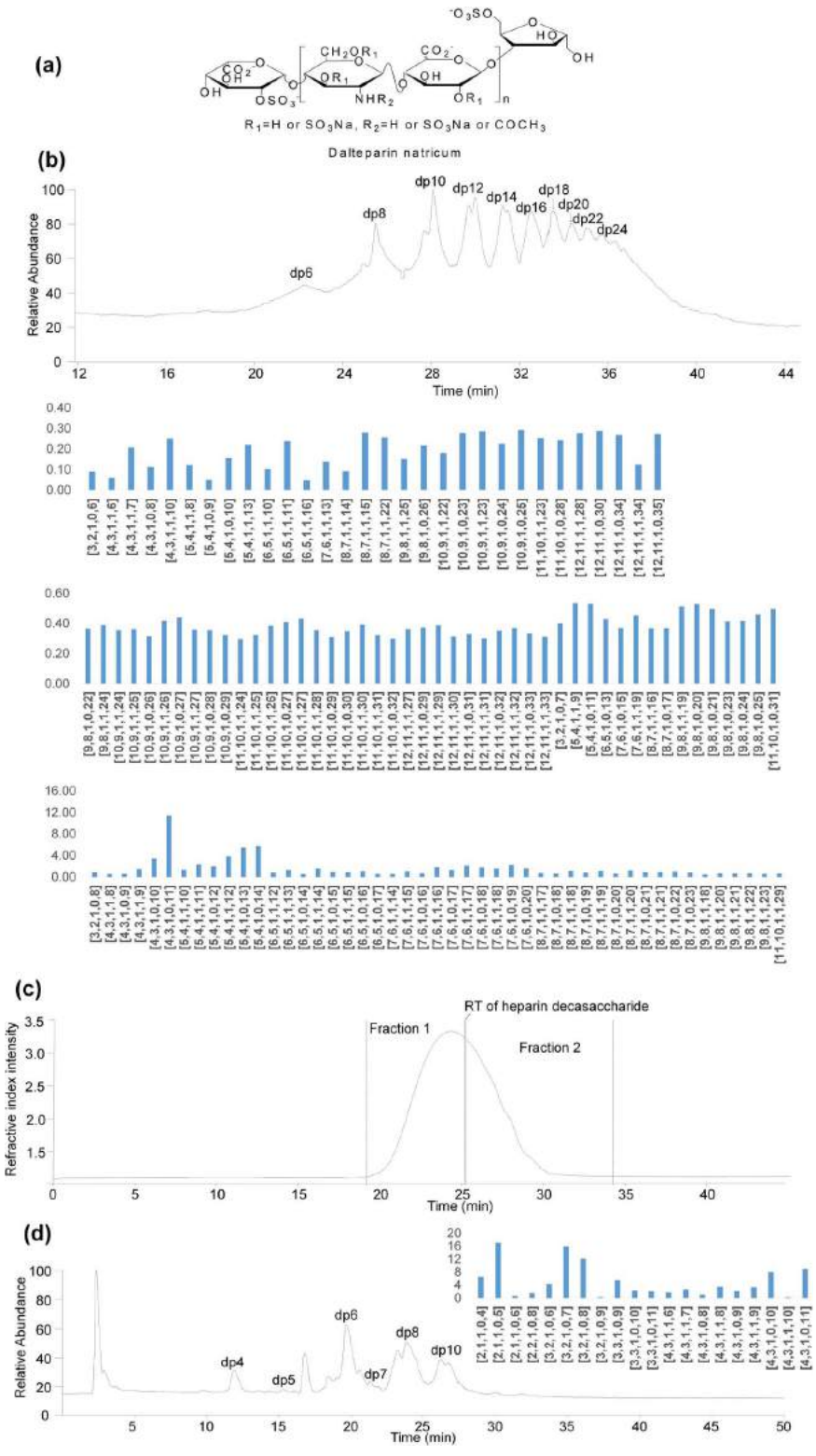

Fig. 1. (**a**) Structure of dalteparin sodium. (**b**) HILIC-ESI–MS total ion chromatogram (TIC) of dalteparin sodium and the oligosaccharide compositions [HexA, GlcN, mannitol, Ac, SO_3]. (**c**) SEC separation of dalteparin. (**d**) HILIC-ESI–MS of the short dalteparin oligosaccharides collected from SEC and the short oligosaccharide compositions.

most difficult molecules to analyze due to its structural complexity and heterogeneity. The chemical modifications during the depolymerization process make the structural elucidation of LMWHs even more challenging.

A great number of analytical methods have been established for structural characterization of heparin and LMWHs from different aspects. Gas chromatography (GC) has been used to determine the monosaccharide constituents of sulfated glycosaminoglycans (Zanetta,

Timmerman, & Leroy, 1999). Gel electrophoresis and capillary electrophoresis (CE) methods have been demonstrated to profile the MW distribution and constituents of LMWHs (Edens, Al-Hakim, Weiler, Rethwisch, Fareed, & Linhardt, 1992; Pervin, Al-Hakim, & Linhardt, 1994; Wang, Reinhard, & Job, 1997). Nuclear magnetic resonance (NMR) technique has exhibited itself as a powerful approach for determining the characteristic terminal structures, monosaccharide composition, substitution patterns and glycosidic linkages of LMWHs (Bisio, Urso, Guerrini, Wit, Torri, & Naggi, 2017; Guerrini, Guglieri, Naggi, Sasisekharan, & Torri, 2007). Various high performance liquid chromatography (HPLC) methods have been developed to analyze the disaccharide composition or oligosaccharide fragments of LMWHs. LMWH oligosaccharides can be separated based on their sizes with a size-exclusion chromatography (SEC) column, which has the limitation to resolve species with different substitutions (Mourier, Agut, Souaifi-Amara, Herman, & Viskov, 2015). Hydrophilic interaction chromatography (HILIC) offers a better resolution than SEC, but it is unable to separate larger oligosaccharides with same size but different sulfation patterns (Skidmore, Guimond, Dumax-Vorzet, Yates, & Turnbull, 2010). Charge based separations, such as strong anion exchange (SAX) and cetyltrimethylammonium (CTA)-SAX, resolve LMWH oligosaccharides carrying different negative charge densities in an effective way (Mourier, Agut, Souaifi-Amara, Herman, & Viskov, 2015; Mourier & Viskov, 2004). Reversed phase (RP) HPLC is not suitable for analysis of LMWHs, but it can be modified by using ion paring reagents to form an ion paring reversed phase chromatography (RPIP) system or label the oligosaccharides with hydrophilic and fluorescent agents to make them retainable on a RP column (Galeotti & Volpi, 2013; Wang, Li, Sun, Bai, Jin, & Chi, 2014; Kinoshita & Sugahara, 1999). Because dalteparin oligosaccharides lack chromophore at the NRE and do not contain reactive RE for fluorescence labelling, a mass spectrometer is necessary to serve as a detector following LC separation. Directly coupling the LC separation to a mass spectrometer (MS) is usually referred as an on-line LC–MS method. Alternatively, the fractions eluted from the LC separation can be collected, selectively combined or desalted, and then injected into a mass spectrometer, which is correspondingly referred as an offline LC–MS method.

In recent years, MS techniques are becoming the mainstay for characterizing oligosaccharides in LMWHs. A top-down and bottom-up strategy, similar to that used in proteomics analysis, has been applied to LMWH analysis. In the top-down approaches, hyphenated techniques, such as SEC (Zhang et al., 2013), RPIP (Li, Chi et al., 2014; Doneanu, Chen, & Gebler, 2009), HILIC (Li, Zhang, Zaia, & Linhardt, 2012) and CE (Sun et al., 2016a,b) coupled with electrospray ionization (ESI)-MS are used to separate LMWH chains and obtain their high-resolution MWs. The structural composition, including numbers of HexA residues, GlcN residues, terminal residues, sulfo group substitutions and *N*-acetyl group substitutions, are then calculated either manually or with the help of bioinformatics tools for individual oligosaccharides with size up to 30 saccharide units (Maxwell et al., 2012). In the bottom-up approaches, LMWHs are either exhaustively digested to disaccharides using a cocktail of heparinase I, II and III for basic building blocks analysis (Wang, Li, Sun, Bai, Jin, & Chi, 2014; Sun et al., 2016a,b) or partially degraded to oligosaccharide fragments by using only one kind of heparinase for fragment mapping analysis (Xu, Li, Chi, Du, Bai, & Chi, 2015; Li, Steppich et al., 2014). The top-down and bottom-up approaches provide in-depth structural elucidation for LMWHs, but both of these MS approaches, along with other technique, such as GC, LC, gel electrophoresis and NMR, pay more attention to the overall structural properties of LMWHs. They are not sufficient to reveal the sequences of these oligosaccharides.

The shorter oligosaccharides in dalteparin are likely to undergo more cleavage reactions than the longer oligosaccharides during the LMWH manufacture process. Therefore, they are more sensitive indicators than other components to reflect the process conditions. Direct sequencing of these shorter oligosaccharides is considered an important aspect for evaluating the structure of LMWHs (Lee et al., 2013). Traditionally, the structural features of heparin oligosaccharides are usually characterized as their MWs and constituents. Recent advances in analytical techniques have made it possible to obtain the complete sequences of LMWH oligosaccharides.

NMR is the usual way to reveal the sequence of a heparin oligosaccharide but has the limitation of requiring substantial amounts of high purity samples. Many attempts have been made to develop sensitive MS methods. For example, in a matrix-assisted laser ionization (MALDI)-MS methodology, basic peptides, such as $(Arg\text{-}Gly)_{19}$-Arg, were used to facilitate the ionization of acidic oligosaccharides. The sequences of heparin-like glycosaminoglycans were denoted by analyzing the intact chains and sequential degraded fragments with high-accuracy MALDI-MS and interpreting the data with a notation system (Venkataraman, Shriver, Raman, & Sasisekharan, 1999). Nowadays ESI–MS is more popular because it can be conveniently coupled with LC or CE. The major challenge of analyzing heparin oligosaccharides with ESI–MS is the neutral loss of sulfo groups, which often occurs during the ionization step and more seriously in the fragmentation process. Co-electrospraying a synthetic heparin pentasaccharide with NaOH can afford more stable species preventing the neutral loss of sulfo groups. Such species are also more highly ionized, which enables more complete glycosidic and cross-ring fragmentations during collision-induced dissociation (CID)-MS/MS analysis (Kailemia, Li, Ly, Linhardt, & Amster, 2012). Heparin oligosaccharides with up to 12 saccharide units and 11 sulfo groups can be fully sequenced using this approach (Kailemia, Li, Xu, Liu, Linhardt, & Amster, 2013). Alternative dissociation techniques, such as electron-detachment dissociation (EDD), also exhibit capabilities of locating the sulfate substitutions and even in distinguishing the HexA residue stereochemistry in heparin-derived tetrasaccharides (Wolff, Chi, Linhardt, & Amster, 2007). Although these achievements in methodology showed great potentials of MS as a sensitive sequencing tool, it is still unrealistic to directly analyze all the oligosaccharides present in a LMWH. Top-down analysis suggests that LMWHs contained many hundreds of different oligosaccharide chain compositions, with the majority of these having sizes larger than 12-mers. Thus, it is wise to focus sequencing on a subset of short oligosaccharide chains instead of broadly focusing on all the components in LMWHs, as smaller chains are likely to have undergone more cleavage reactions than the longer chains and, thus, serve as more sensitive indicators of the depolymerization process conditions (Lee et al., 2013). The tetrasaccharide pool of enoxaparin sodium has been sequenced by orthogonal experiments, including fractionating tetrasaccharides using SEC, purifying individual chains using semi-preparative SAX-HPLC and characterizing each component with MALDI-MS and NMR (Ozug et al., 2012). However, the short oligosaccharides in dalteparin sodium cannot be analyzed using the same approach. Unlike enoxaparin, dalteparin chains do not have chromophores that can be easily monitored during the chromatographic separation. Additionally, the MW of dalteparin is larger than enoxaparin, and the major components in the short oligosaccharide pool of dalteparin are hexasaccharides and octasaccharides, rather than the tetrasaccharides found in enoxaparin. The increased size of dalteparin chains make it unpractical to obtain individual dalteparin oligosaccharides of satisfactory purity for NMR analysis.

In this study, we developed an offline SAX-HPLC and ESI–MS/MS approach for sequencing the short oligosaccharide pool of dalteparin sodium. The oligosaccharides with sizes equal or smaller than octasaccharides were separated from dalteparin using SEC. These chains were further separated using high resolution SAX-HPLC column. The fractions were desalted and determined by ESI–MS. Finally, the individual chains were sequenced using optimized MS/MS conditions. This work provides a sensitive and indispensable tool to evaluate the fine structures of LMWHs that can be used in conjunction with top-down and bottom-up chain mapping approaches.

2. Materials and methods

2.1. Materials

Dalteparin reference standard was obtained from the European Pharmacopoeia. Heparin disaccharide standard ΔIVA (ΔUA-GlcNAc) was purchased from Iduron (Manchester, UK). Heparin lyase I, II, and III were obtained from Aglyco (Beijing, China). Arixtra™ was obtained from the hospital pharmacy. HPLC grade acetonitrile, methanol and water were from Fisher-Scientific (Springfield, NJ). All other reagents and chemicals were of the purest grade available.

2.2. SEC separation

The short oligosaccharides were separated by SEC with a Superdex TM Peptide 10/300 GL column (13 μm, 10 × 300 mm) from GE Healthcare (Uppsala, Sweden) on an LC-20A HPLC system (Shimadzu, Kyoto, Japan) equipped with a refractive index detector. Isocratic mobile phase of 0.2 M ammonium bicarbonate was used at the flow rate of 0.4 mL/min. The short oligosaccharide pool was collected and the volatile salts were removed by repeated lyophilization.

2.3. SAX separation

The short oligosaccharide pool was further separated on a ProPac PA1 SAX column (4 × 250 mm) from Thermo Scientific (Barrington, IL). Mobile phase A was 0.2 M NaCl, pH 7.0 and mobile phase B was 2 M NaCl, pH 7.0. A step gradient of 0% mobile phase B in 5 min, from 0 to 30% B in 45 min, from 30 to 85% B in 150 min and from 85 to 100% B in 10 min was used. The flow rate was at 1 mL/min. The eluents were collected using an automatic fraction collector by setting as 1 min/tube and collecting from 0 min to 120 min. The fractions were then desalted using a Sephadex G-10 column (10 × 400 mm) from Dalian Elite (Dalian, China). Equal volume of disaccharide standard ΔIVA (0.08 μg/μL) was added to each fraction before desalting to serve as an internal standard.

2.4. ESI–MS and MS/MS analysis

Each desalted fraction dissolved in 30 μL water was directly introduced to the ESI–MS interface of a Thermo LTQ-Orbitrap XL mass spectrometer (Thermo Fisher Scientific, San Jose, CA). The negative ion mode was used with the sheath gas flow rate at 20 arb; aux gas flow rate at 5 arb; I spray voltage at 3.5 KV; capillary temp at 275.00 °C; capillary voltage at −40.00 V and tube lens at −50.00 V. For MS/MS analysis of representative oligosaccharides, the samples were subjected to ESI–MS at a concentration of 0.5–1 μg/μL in 50% methanol containing 2–5 mM NaOH. The parameters of first stage MS were the same as above. The MS/MS parameters were set as following: Iso width (m/z), 3.0; normalized collision energy, 50.0 or 55.0.

2.5. Sequence assignment using python 2.7 software

A program was written in Python to facilitate the interpretation of MS/MS spectra. It included two compartments, database and fitting algorithm. The theoretical fragment ion database was generated for each oligosaccharide according to its composition. A fitting algorithm with 0.02 Da mass acceptance range was used to match the experimental fragment ions by searching against the theoretical fragment ion database.

2.6. Enzymatic digestion and LC–MS/MS analysis

A digestion solution was prepared by mixing 12.5 μL of 0.4 IU/mL each of heparinase I, II and III with 8.75 μL of sodium acetate/calcium acetate buffer (pH 7.0). The oligosaccharide was digested into disaccharide blocks by incubating at 37 °C for 24 h. The digest was then analyzed using an Agilent 1100 capillary HPLC system (Agilent Technologies, Santa Clara, CA) coupled to a Thermo LTQ-Orbitrap Velos Pro mass spectrometer (Thermo Fisher Scientific, San Jose, CA). The column was a Phenomenex Luna HILIC column (2 × 150 mm, 200 Å, Torrance, CA). Mobile phase A was 5 mM ammonium acetate aqueous solution, while mobile phase B was 5 mM ammonium acetate in 95% acetonitrile. A gradient elution with 95% mobile phase B in 5 min, followed by 95–77% B in 102 min, was used at a flow rate of 0.15 mL/min. The mass spectrometer was operated in the negative ion mode with the following parameters: sheath gas flow rate (arb), 10; auxiliary gas flow rate (arb), 2; spray voltage, 3.5 kV; capillary temperature, 275.00 °C; S-lens level, 10%. The MS/MS parameters were the same as above.

3. Results and discussion

3.1. Separation of short oligosaccharide pool from dalteparin

Dalteparin is comprised of a broad range of nitrous acid depolymerized heparin oligosaccharides, with a typical mass-average relative molecular mass of 6000 Da. A reference standard sample from the European Pharmacopoeia was analyzed using HILIC-ESI–MS to profile the chain distribution of dalteparin. A total of 123 chain compositions were determined (Fig. 1b). Hexasaccharides and octasaccharides were the main components of the short oligosaccharide pool, while minor oligosaccharides with degree of depolymerization (dp4), dp5 and dp7 with different sulfo group substitutions, were also detected. The short oligosaccharide pool was next separated from dalteparin using SEC equipped with a refractive index detector. The retention time of a decasaccharide was chosen as the cutoff point to ensure all octasaccharides were included in Fraction 2 (Fig. 1c). The fractions were desalted and re-analyzed using the HILIC-MS method to demonstrate the completeness of collecting short oligosaccharides. In Fraction 1, no oligosaccharide with size equal or smaller than dp8 was detected, while 20 different compositions from dp4 to dp8 were determined in Fraction 2 by matching the high resolution MW (Fig. 1d). Some larger oligosaccharides, such as dp9 and dp10, were also collected in this fraction, but they were not subjected to the sequencing analysis.

3.2. Further separation of oligosaccharides using SAX-HPLC

Although the HILIC column was able to separate dalteparin oligosaccharides of different compositions, it incompletely resolves isomers with the same molecular formula but different sulfo group and *N*-acetyl group substitution pattern or stereoisomers having different HexA chirality. RPIP can separate heparin oligosaccharide isomers to some extent, but the ion pairing reagents are difficult to remove and can interfere in the MS/MS fragmentations (Li, Chi et al., 2014; Doneanu et al., 2009). SAX is the traditional way to separate acidic oligosaccharides. A ProPac PA1 SAX column has been used to separate LMWH oligosaccharides and gives the best resolution (Ozug et al., 2012). The dalteparin oligosaccharides are not detectable by the UV detector due to the lack of a chromophore or by using a refractive index detector because of the salt gradient required for their elution. The high concentration of salts in the mobile phase also precludes the direct infusion of the SAX column eluent into the ESI interface. Thus, we developed an off-line SAX and ESI–MS approach to further separate the short oligosaccharide pool of dalteparin. The eluents were collected every minute by an automatic fraction collector and equal amount of heparin disaccharide ΔIVA was added to each fraction. Following desalting, each fraction was analyzed by ESI–MS to identify the components and determine their relative quantities in comparison with the internal standard. The SAX chromatogram was then plotted and shown in Fig. 2a. All the short oligosaccharides detected in the HILIC-ESI–MS analysis were found again in the SAX analysis. In addition, some minor

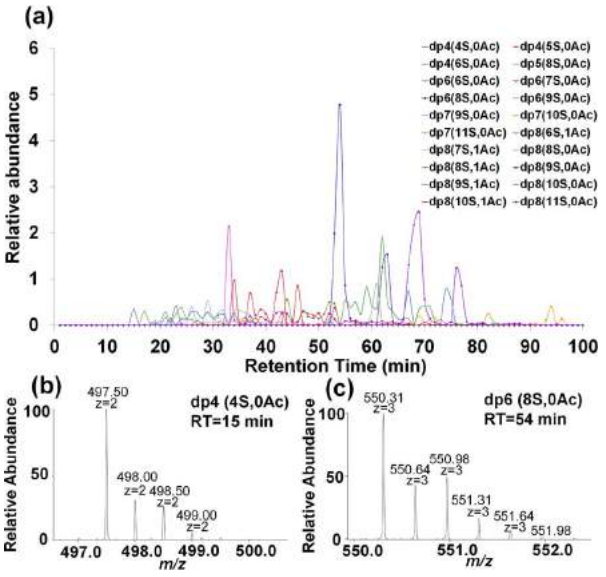

Fig. 2. (**a**) Extracted ion chromatogram (EIC) of each detected dalteparin oligosaccharide. (**b**) The zoomed mass spectrum of isotopic peaks of dp4 (5S, 0Ac). (**c**) The zoomed mass spectrum of isotopic peaks of dp6 (8S, 0Ac).

Table 1
The major components identified from the dalteparin short oligosaccharide pool by off-line SAX and ESI–MS analysis.

Number	Composition	Major ions observed	*m/z*	Retention time (min)
1	dp4 (4S, 0Ac)	$[M-2H]^{2-}$	497.5034	15
2	dp4 (5S, 0Ac)	$[M-2H]^{2-}$	537.4828	33
3	dp4 (6S, 0Ac)	$[M-2H]^{2-}$	577.4609	43
4	dp5 (8S, 0Ac)	$[M-3H]^{3-}$	491.6310	82
5	dp6 (6S, 0Ac)	$[M-3H]^{3-}$	497.0043	26, 29, 32, 35
6	dp6 (7S, 0Ac)	$[M-3H]^{3-}$	529.3316	34, 37, 43, 46
7	dp6 (8S, 0Ac)	$[M-3H]^{3-}$	550.3098	54, 63
8	dp6 (9S, 0Ac)	$[M-3H]^{3-}$	576.9600	73
9	dp7 (9S, 0Ac)	$[M-3H]^{3-}$	630.6498	61
10	dp7 (10S, 0Ac)	$[M-3H]^{3-}$	651.626	69, 72
11	dp7 (11S, 0Ac)	$[M-3H]^{3-}$	683.9568	94, 96
12	dp8 (6S, 1Ac)	$[M-3H]^{3-}$	623.3771	17, 21, 24
13	dp8 (7S, 1Ac)	$[M-4H]^{4-}$	487.2678	26, 29, 32
14	dp8 (8S, 0Ac)	$[M-3H]^{3-}$	668.3496	31
15	dp8 (8S, 1Ac)	$[M-3H]^{3-}$	676.6803	44, 52
16	dp8 (9S, 0Ac)	$[M-3H]^{3-}$	689.3276	43, 47, 50, 52
17	dp8 (9S, 1Ac)	$[M-3H]^{3-}$	709.0069	67, 74
18	dp8 (10S, 0Ac)	$[M-3H]^{3-}$	715.9792	55, 59, 62
19	dp8 (10S, 1Ac)	$[M-3H]^{3-}$	729.9813	79
20	dp8 (11S, 0Ac)	$[M-3H]^{3-}$	742.6305	69, 76

components not previously detected were discovered after they eluted separately from the abundant species. The SAX column also showed good capability of resolving isomers, for examples, the oligosaccharide with composition of dp6 (7S, 0Ac) eluted at 4 different retention times, 34 min, 37 min, 43 min and 46 min, and the oligosaccharide dp8 (10S, 0Ac) gave two peaks at 59 min and 62 min. The molecular compositions and retention times of all short oligosaccharides are summarized in Table 1. Representative oligosaccharide species present in relatively high abundance were selected from this table for sequence analysis.

3.3. Optimization of ESI–MS/MS conditions

ESI–MS/MS is one of the most sensitive tools to sequence the highly negatively charged heparin oligosaccharides. However, the sequence information obtained is limited due to the neutral loss of sulfo groups. The Amster group discovered that the neutral loss of sulfo groups could be minimized by adding sodium hydroxide to deprotonate all acidic groups on the oligosaccharides (Kailemia et al., 2012). They have successfully sequenced a chemically synthesized heparin pentasaccharide and a series of biochemically synthesized heparan sulfate oligosaccharides with sizes up to dp12 (Kailemia et al., 2013). However, the Fourier transform ion cyclotron resonance (FT-ICR) mass spectrometer used in their research is not readily accessible in most laboratories. In contrast the readily accessible LTQ-Orbitrap mass spectrometer, operating in the CID mode, failed to sufficiently fragment the oligosaccharide (Kailemia et al., 2012). We optimized the ESI–MS/MS conditions on an LTQ-Orbitrap XL mass spectrometer using a synthetic heparin pentasaccharide, Arixtra™. Arixtra™ has a known sequence of GlcNS6S-GlcA-GlcNS6S3S-IdoA2S-GlcNS6S-OCH_3. First, the electrospray parameters were optimized to achieve the highest sensitivity without obvious loss of sulfo groups. At the spray voltage of −3.5 KV and capillary temperature of 275 °C, sufficient parent ions with complete deprotonation of all acidic groups were generated by infusing Arixtra™ with 1 mM NaOH, and the three most abundant peaks were $[M-10H+7Na]^{3-}$, $[M-10H+6Na]^{4-}$ and $[M-10H+5Na]^{5-}$. According to the literature, combining the fragment ions from these parent ions with different charge states allows the determination of the full sequence of Arixtra™. Next, the dissociation parameters were investigated. At the normalized collision energy of 55%, enough glycosidic and cross-ring fragmentations were formed with minimal loss of sulfo groups. The lowest amount of sample required for obtaining the full sequence of Arixtra™ was 1 μg using the regular ESI interface and 100 ng using the nanoESI (see Supplementary Fig. S1).

3.4. Development of computer-assisted MS/MS spectra interpretation tool

Heparin oligosaccharides can generate hundreds of fragment ions using CID, and it normally takes quite a few hours for an experienced analyst to assign the spectra and deduce a sequence. A program was developed using Python 2.7 to facilitate the interpretation of MS/MS spectra. When the composition of an oligosaccharide is obtained by high-resolution ESI–MS, all theoretical sequences with different possible sulfation and *N*-acetylation patterns were automatically generated. A database containing all likely fragmentations as well as various sodium adductions, corresponding to these sequences, was established. The workflow of using this tool to interpret the MS/MS results for Arixtra™ is shown in Supplementary Fig. S2. It took only a few minutes to accurately assign the spectra and export the correct sequence.

3.5. Sequencing oligosaccharides in dalteparin

Eighteen representative oligosaccharides were selected for ESI–MS/MS and sequence analysis (Table 2). The optimized experimental conditions, obtained by infusing Arixtra™, were used for analyzing dalteparin short oligosaccharides. The concentration of NaOH in the electrospray solution was adjusted according to the chain length and sulfation degree of each oligosaccharide to ensure the parent ions were fully deprotonated

Octasaccharides are the largest oligosaccharides to be analyzed. According to the definition of dalteparin (Fig. 1a), an octasaccharide can have up to 11 sulfo groups. Oligosaccharide **1** with the composition dp8 (11S, 0Ac) is the fully sulfated form and its sequence was successfully determined. Three precursor ions with all 15 acidic protons replaced by Na^+, m/z = 403.79, −6 charged, m/z = 489.14, −5 charged, and m/z = 617.17, −4 charged, were subjected to CID analysis to yield complementary fragment ions. Glycosidic bond cleavage fragment ions were used to assign sulfo and *N*-acetyl groups to each monosaccharide residue, and the cross-ring cleavage fragment ions were helpful to locate the substitution position of sulfo groups within each monosaccharide residue. For example, Y_6 and Y_5 ions demonstrated that one sulfo group was located at residue f, and the $^{0,2}X_5$ ion

Table 2
Representative oligosaccharide species for sequencing analysis.

Oligosaccharide No.	Composition	Retention Time (min)	Sequence
1	dp8 (11S, 0Ac)	76	HexA2S-GlcNS3S/6S-HexA2S-GlcNS6S-HexA2S-GlcNS3S/6S-HexA2S-Mnt6S-2,5-anhydro
2	dp8 (11S, 0Ac)	69	HexA2S-GlcNS6S-HexA2S-GlcNS3S/6S-HexA2S-GlcNS6S-HexA2S-Mnt6S-2,5-anhydro
3	dp8 (10S, 0Ac)	62	HexA2S-GlcNS6S-HexA-GlcNS6S-HexA2S-GlcNS6S-HexA2S-Mnt6S-2,5-anhydro
4	dp8 (10S, 0Ac)	59	HexA2S-GlcNS6S-HexA2S-GlcNS6S-HexA2S-GlcNH$_2$6S-HexA2S-Mnt6S-2,5-anhydro
5	dp8 (9S, 0Ac)	50	HexA2S-GlcNS6S-HexA-GlcNS6S-HexA2S-GlcNS3S/6S-HexA-Mnt6S-2,5-anhydro
6	dp8 (9S, 1Ac)	74	HexA2S-GlcNS6S-HexA-GlcNAc6S-HexA2S-GlcNS3S/6S-HexA2S-Mnt6S-2,5-anhydro
7	dp6 (8S, 0Ac)	54	HexA2S-GlcNS6S-HexA2S-GlcNS6S-HexA2S-Mnt6S-2,5-anhydro
8	dp6 (8S, 0Ac)	63	HexA2S-GlcNS3S/6S-HexA2S-GlcNS6S-HexA2S-Mnt6S-2,5-anhydro
9	dp6 (9S, 0Ac)	73	HexA2S-GlcNS3S/6S-HexA2S3S-GlcNS3S/6S-HexA2S-Mnt6S-2,5-anhydro
10	dp6 (7S, 0Ac)	34	HexA2S-GlcNS6S-HexA2S-GlcNS-HexA2S-Mnt6S-2,5-anhydro
11	dp6 (7S, 0Ac)	43	HexA2S-GlcNS3S/6S-HexA-GlcNS6S-HexA2S-Mnt6S-2,5-anhydro
12	dp6 (7S, 0Ac)	46	HexA2S-GlcNS-HexA2S-GlcNS6S-HexA2S-Mnt6S-2,5-anhydro
13	dp4 (5S, 0Ac)	33	HexA2S-GlcNS6S-HexA2S-Mnt6S-2,5-anhydro
14	dp4 (4S, 0Ac)	15	HexA2S-GlcNS6S-HexA-Mnt6S-2,5-anhydro
15	dp7 (11S, 0Ac)	94	GlcNS3S/6S-HexA2S-GlcNS6S-HexA2S-GlcNS6S-HexA2S-Mnt6S-2,5-anhydro
16	dp7 (10S, 0Ac)	69	GlcNS3S/6S-HexA2S-GlcNS6S-HexA2S-GlcNS6S-HexA2S-Mnt6S-2,5-anhydro
17	dp7 (9S, 0Ac)	61	GlcNS3S/6S-HexA2S-GlcNS-HexA2S-GlcNS3S/6S-HexA2S-Mnt6S-2,5-anhydro
18	dp5 (8S, 0Ac)	82	GlcNS3S/6S-HexA2S-GlcNS3S/6S-HexA2S-Mnt6S-2,5-anhydro

provided further evidence to identify it as a 2-*O*-sulfation. The mass difference between Y_5 and Y_4 ions deduced that residue e contained an *O*-sulfo and an *N*-sulfo group, and the *O*-sulfo group can be further identified as a 6-*O*-sulfation by the presence of $^{2,4}A_4$ ion. The sequence of oligosaccharide **1** was deduced as HexA2*S*-GlcNS3*S*/6*S*-HexA2*S*-GlcNS6*S*-HexA2*S*-GlcNS3*S*/6*S*-HexA2*S*-Mnt6*S*-2,5-anhydro (Fig. 3a). Oligosaccharide **2** has the same composition as oligosaccharide **1**, and the ESI–MS/MS result revealed its sequence as HexA2*S*-GlcNS6*S*-HexA2*S*-GlcNS3*S*/6*S*-HexA2*S*-GlcNS6*S*-HexA2*S*-Mnt6*S*-2,5-anhydro.

The distributions of fragment ions were apparently different between oligosaccharide **1** and **2,** suggesting they are likely to be isomers with different HexA epimerization or different 3-*O*-sulfation on the GlcN residues (Fig. 3b). Some signature cross-ring fragment ions are known to be able to differentiate iduronic and glucuronic acid epimers of synthetic heparin oligosaccharides (Kailemia et al., 2012; Kailemia et al., 2013). However, the determination of epimers was not successful in the case of oligosaccharides separated from this complex mixture. In addition, when 3-*O*-sulfation occurs on the GlcN residues, the formation of cross-ring fragment ions is impeded because that 3-*O*-hydrogen on GlcN residue is prerequisite for the formation of $^{0,2}A_n$ and $^{2,4}A_n$ product ions (Kailemia et al., 2013). Oligosaccharide **3** and **4** are another pair of isomers with one less sulfo groups compared to the fully sulfated form. Their MS/MS spectra were shown in Supplementary Fig. S3c and S3d . The fragment ions Y_1, Y_2, Y_3 and Z_4 of oligosaccharide **3** had the same *m/z* values as those of oligosaccharide **1** and **2**, suggesting that they bore the same sulfation pattern from residue a to d. The mass differences between Y_6 and Y_5 as well as C_3 and C_2 provided sufficient evidence that residue f was not sulfated (Fig. 3c). For oligosaccharide **4**, the undersulfation was located on the *N*-position of residue c, proved by the ions $^{2,4}A_6$, $^{0,2}A_6$ and Y_2 (Fig. 3d). Therefore, oligosaccharide **3** and **4** are isomers with different sulfation pattern. The sequences of oligosaccharide **5** and **6** were also delineated (Fig. 3e and 3f). Oligosaccharide **6** contained one *N*-acetyl group, and it was allocated on residue e by fragment ions B_4 and $^{0,2}A_4$.

The subgroup of hexasaccharides was analyzed using the same approach. Oligosaccharide **7** and **8** are the fully sulfated hexasaccharide isomers with composition of dp6 (8S, 0Ac). The sequence of oligosaccharide **7** was revealed as HexA2S-GlcNS6S-HexA2S-GlcNS6S-HexA2S-Mnt6S-2,5-anhydro, while oligosaccharide **8** differed from **7** either by uronic acid residue epimerization or sulfation pattern on residue e. No cross-ring fragmentation was observed on this residue, which leaves two possibilities of 6-*O*-sulfation or 3-*O*-sulfation (Fig. 4a and b). Surprisingly, oligosaccharide **9** contained one extra sulfo group over the fully sulfated dalteparin hexasaccharide. The Δmass between B_4 and B_2 ions indicated that the excess sulfo group was located at the disaccharide residue c and d. Additionally, fragment ions Y_3 and Y_2 provided complementary information and allowed to narrow down two sulfo groups within the HexA residue d (Fig. 4c). Although no cross-ring fragmentation occurred in this residue, these two sulfo groups could be assigned at the 2-*O* and 3-*O*-positions because these are the only two available places for *O*-sulfate substitutions. To further confirm this novelty structure, we depolymerized oligosaccharide **9** with heparinases and analyzed its basic constituents using LC–MS/MS. (See Section 3.6). The undersulfated hexasaccharide dp6 (7S, 0Ac) showed more variable sulfation patterns. Four isomers were eluted at different retentions times from the SAX column (Table 1), and three of them were abundant enough for ESI–MS/MS analysis. Compared to the sequence of fully sulfated oligosaccharide **7**, the one fewer sulfate group in oligosaccharide **10**, **11** and **12** could be determined by corresponding characteristic fragment ions. As shown in Fig. 4d and Supplementary Fig. S4d, the $[Y_3 + 2Na]^{2-}$ and $[Y_2 + Na]^{2-}$ ions indicated that the undersulfation of oligosaccharide **10** was on residue c. The B_4 and $^{2,4}A_4$ ions disclosed that the 6-*O*-position was unsulfated instead of the *N*-position. Similarly, oligosaccharide **11** and **12** were unambiguously identified to be the 2-*O*-desulfated on residue d and 6-*O*-desulfated on residue e by ions $[^{0,2}X_3 + 3Na]^{2-}$ and $[Y_3 + 4Na]^{-}$ and ions $[Z_4 + 2Na]^{2-}$, Y_5, Z_4 and $^{0,2}A_2$, respectively (Fig. 4e, f, Supplementary Fig. S4e and S4f).

Tetrasaccharides were the shortest chains found in dalteparin. Two species with different degrees of sulfation were sequenced and their annotated MS/MS spectra were shown in Supplementary Fig. S5. Besides these even numbered oligosaccharides, components with odd number of sugar residues, including three heptasaccharides and one pentasaccharide, were also present in the short oligosaccharide pool of dalteparin. Odd numbered oligosaccharides were reported in enoxaparin as byproducts from peeling reaction (Liverani, Mascellani, & Spelta, 2009). However, the borohydride reduction step in the process of dalteparin has already protected the RE of oligosaccharide chains from peeling reaction. All four odd numbered oligosaccharides have an additional GlcN residue at their NRE. Interestingly, MS/MS results suggested that all the terminal GlcN residues were substituted or likely substituted by 3-*O*-sulfo group. 3-*O*-sulfation of GlcN residue is a unique structure in heparin and responsible for many important bioactivities including the anticoagulant activity. While the nitrous acid prefers to cleave the 1→4 linkages between GlcN and HexA residues and forms even numbered oligosaccharides, the 3-*O*-sulfation of GlcN residue may cause the glycosidic bond between HexA and GlcN3S residue more cleavable and result in odd numbered oligosaccharides. The annotated MS/MS spectra of odd numbered oligosaccharides are presented in Supplementary Fig. S6. This provides a novel insight in understanding

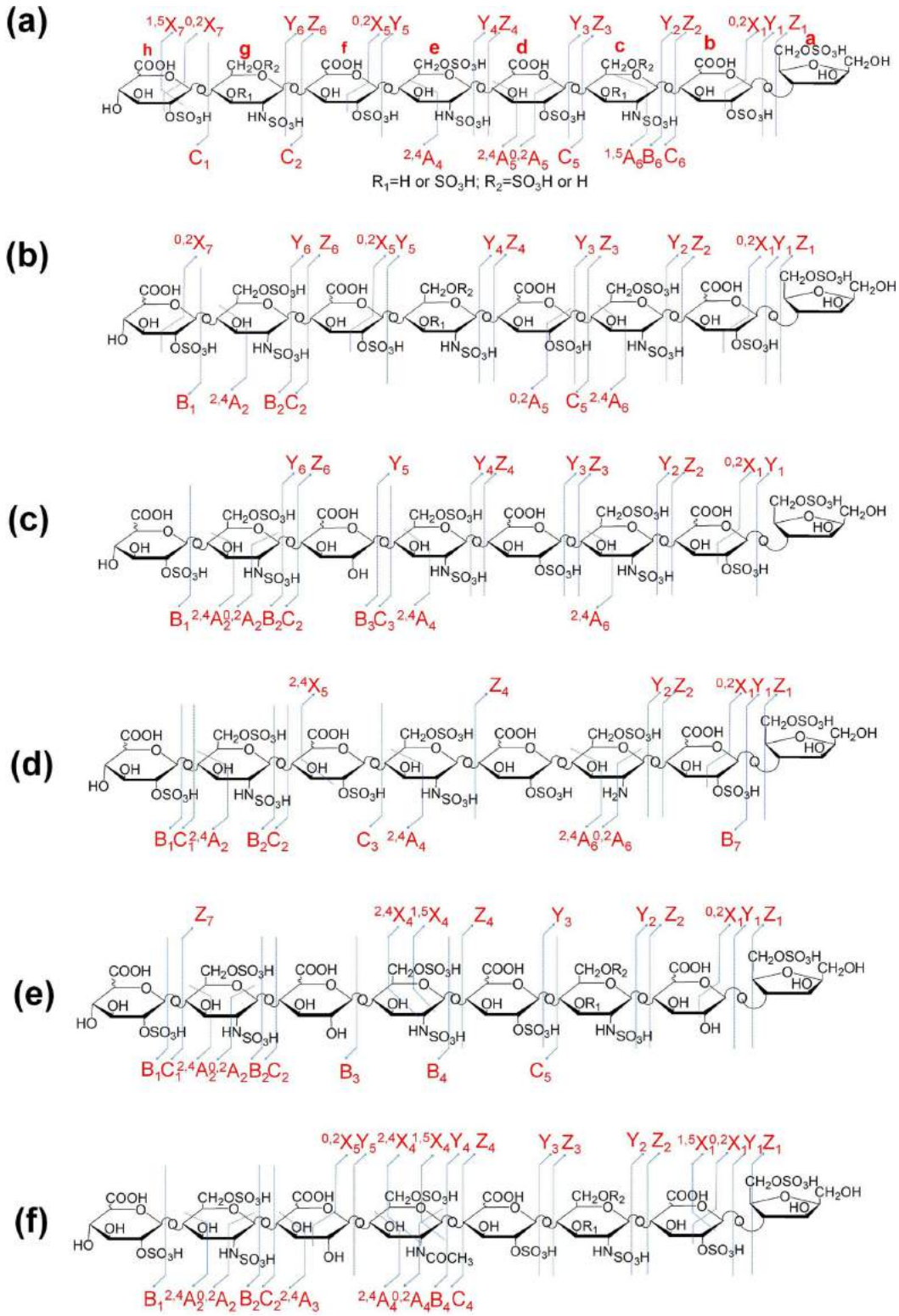

Fig. 3. The annotated sequences of dalteparin octasaccharides obtained from CID-MS/MS analysis. (**a**) Oligosaccharide **1.** (**b**) Oligosaccharide **2.** (**c**) Oligosaccharide **3.** (**d**) Oligosaccharide **4.** (**e**) Oligosaccharide **5** and (**f**) Oligosaccharide **6.** The CID-MS/MS spectra of fragmenting fully deprotonated precursor ions with different charge states are presented in Supplementary Fig. S3.

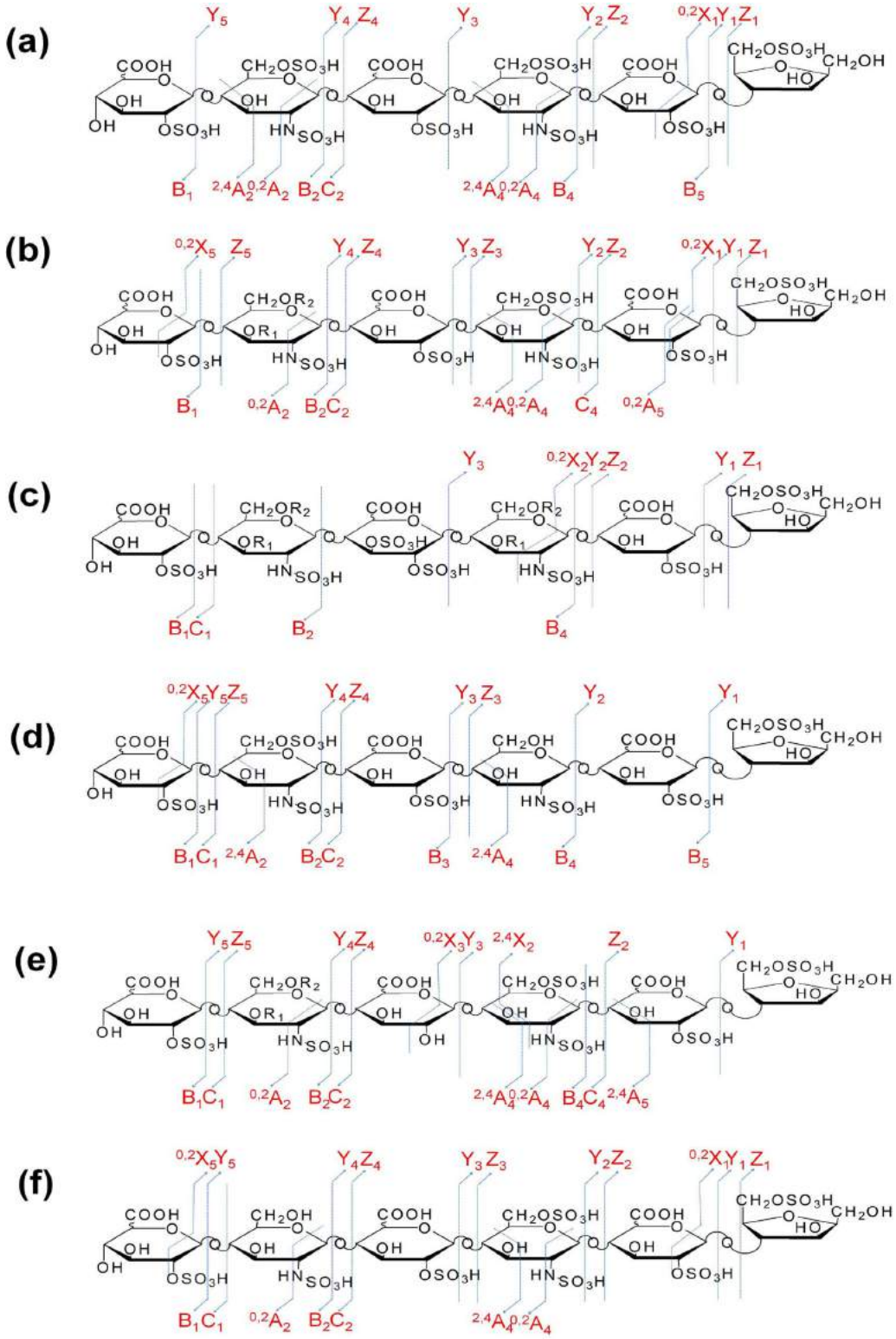

Fig. 4. The annotated sequences of dalteparin hexasaccharides obtained from CID-MS/MS analysis. (**a**) Oligosaccharide **7**. (**b**) Oligosaccharide **8**. (**c**) Oligosaccharide **9**. (**d**) Oligosaccharide **10**. (**e**) Oligosaccharide **11** and (**f**) Oligosaccharide **12.** The CID-MS/MS spectra of fragmenting fully deprotonated precursor ions with different charge states are presented in Supplementary Fig. S4.

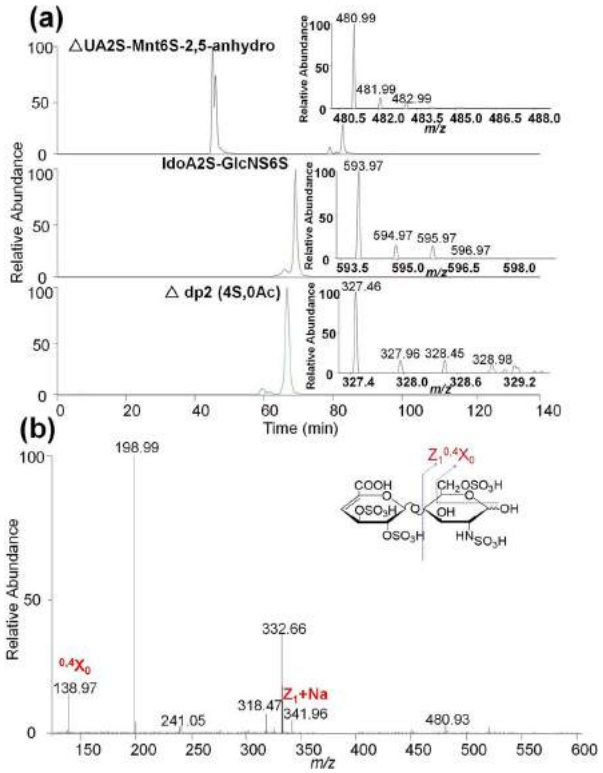

Fig. 5. (**a**) HILIC-ESI–MS analysis of the enzymatic digest of oversulfated hexasaccharide and the zoomed MS spectra of three disaccharide blocks. (**b**) CID-MS/MS spectrum of Δdp2 (4S, 0Ac), precursor ion $[M\text{-}5H + 3Na]^{2-}$.

the reaction mechanism of dalteparin process that is distinct from other types of LMWHs.

3.6. Confirmation of unusual 3-O-sulfated HexA structure using enzymatic digestion and LC–MS/MS

In the ESI–MS/MS sequencing analysis, oligosaccharide **9**, a hexasaccharide containing unusual 2,3-*O*-disulfated HexA residue, was discovered. However, 3-*O*-sulfation was known to only occur on the GlcN residue by 3-*O*-sulfotransferases during the biosynthesis of heparin (Wang et al., 2017). Oligosaccharide **9** was digested with a cocktail of heparinase I, II, III and analyzed using LC–MS/MS to provide more evidence for the presence of this unusual structure. Three enzymatically-digested disaccharides were detected which enable reconstruction of the sequence of the parent hexasaccharide: the disaccharide ΔHexA2*S*-Mnt6*S*-2,5-anhydro from the RE, the disaccharide Δdp2 (4S, 0Ac) from the middle and the disaccharide HexA2S-GlcNS6S from the NRE (Fig. 5a). The disaccharide Δdp2 (4S, 0Ac) was subjected to ESI–MS/MS analysis. As presented in Fig. 5b, CID fragmentation of the fully deprotonated precursor ion $[M\text{-}5H + 3Na]^{2-}$ generated two signature fragment ions $^{0,4}X_0$ (m/z = 138.97) and $[Z_1 + Na]^-$ (m/z = 341.95), which indicated that there were two sulfo groups on the residue at the RE and the rest two sulfo groups should be on the ΔHex residue. The direct sequencing and enzymatic digestion analysis results provided sufficient evidence that oligosaccharide **9** contains a 3-*O*-sulfated HexA structure, which has never been reported in dalteparin. Previous basic building block analysis of dalteparin also disclosed a 3-*O*-sulfated HexA residue containing tetrasaccharide, ΔUA-GlcNS-HexA2S3S-GlcNS (Sun et al., 2017). Multiple tests of dalteparin from different aspects have consistently identified and quantified the 3-*O*-sulfated HexA structure, suggesting that it does exist in dalteparin.

Interestingly, our group had previously discovered the ΔUA-GlcNS-HexA2S3S-GlcNS tetrasaccharide in the bottom-up analysis of enoxaparin (Sun et al., 2016a,b). Since the two types of LMWHs are produced though different chemical reactions, the 3-*O*-sulfation is very possibly a natural modification in heparin. The biosynthesis pathway and function of this novel sulfation pattern of heparin are worth further investigation.

4. Conclusions

Although comprehensive characterization of LMWHs has been widely performed by using integrated analytical methods such as HPLC, CE, LC–MS and NMR, the structural information provided by these approaches is not sufficient to monitor the efficacy and safety of LMWHs drugs. Direct sequencing of oligosaccharides provides straightforward assessment of the structural microheterogeneity for LMWH drugs, and the short oligosaccharide pool is the most sensitive indicator to the depolymerization reaction conditions. While obtaining pure oligosaccharide chains from such complex mixture as LMWHs is still not practical, ESI–MS/MS offers a timely solution with low sample consumption, low requirement of sample purity but rich structural information. In addition, ESI–MS unbiasedly evaluates the oligosaccharides in LMWHs no matter they contain a chromophore or not. Herein, we developed an offline SAX-ESI–MS/MS approach and demonstrated the sequencing of representative short oligosaccharides with relatively high abundance in dalteparin. Sequencing the minor components is also feasible by accumulating enough samples from multiple runs, developing high throughput desalting method and using the more sensitive nanoESI interface.

Acknowledgments

This work was supported by grant from the National Natural Science Foundation of China (21472115) and the National Key Research and Development Program of China (2017YFF0205404).

Appendix A. Supplementary data

Supplementary data associated with this article can be found, in the online version, at http://dx.doi.org/10.1016/j.carbpol.2017.11.039.

References

Ahmed, I., Majeed, A., & Powell, R. (2007). Heparin induced thrombocytopenia: diagnosis and management update. *Postgraduate Medical Journal, 83*, 575–582.
Bisio, A., Vecchietti, D., Citterio, L., Guerrini, M., Raman, R., Bertini, S., et al. (2009). Structural features of low-molecular-weight heparins affecting their affinity to antithrombin. *Thrombosis and Haemostasis, 102*, 865–873.
Bisio, A., Urso, E., Guerrini, M., Wit, P. D., Torri, G., & Naggi, A. (2017). Structural characterization of the low-molecular-weight heparin dalteparin by combining different analytical strategies. *Molecules, 22*, E1051.
Chuang, Y. J., Swanson, R., Raja, S. M., & Olson, S. T. (2001). Heparin enhances the specificity of antithrombin for thrombin and factor Xa independent of the reactive center loop sequence. *Journal of Biological Chemistry, 276*, 14961–14971.
Doneanu, C. E., Chen, W., & Gebler, J. C. (2009). Analysis of oligosaccharides derived from heparin by ion-pair reversed-phase chromatography/mass spectrometry. *Analytical Chemistry, 81*, 3485–3499.
Edens, R. E., Al-Hakim, A., Weiler, J. M., Rethwisch, D. G., Fareed, J., & Linhardt, R. J. (1992). Gradient polyacrylamide gel electrophoresis for determination of molecular weights of heparin preparations and low-molecular-weight heparin derivatives. *Journal of Pharmaceutical Sciences, 81*, 823–827.
Galeotti, F., & Volpi, N. (2013). Novel reverse-phase ion pair-high performance liquid chromatography separation of heparin, heparan sulfate and low molecular weight-heparins disaccharides and oligosaccharides. *Journal of Chromatography A, 1284*, 141–147.
Gray, E., Mulloy, B., & Barrowcliffe, T. W. (2008). Heparin and low-molecular-weight heparin. *Thrombosis and Haemostasis, 99*, 807–818.
Guerrini, M., Guglieri, S., Naggi, A., Sasisekharan, R., & Torri, G. (2007). Low molecular weight heparins: structural differentiation by bidimensional nuclear magnetic resonance spectroscopy. *Seminars in Thrombosis and Hemostasis, 33*, 478–487.
Hirsh, J., & Levine, M. N. (1992). Low molecular weight heparin. *Blood, 79*, 1–17.
Kailemia, M. J., Li, L., Ly, M., Linhardt, R. J., & Amster, I. J. (2012). Complete mass spectral characterization of a synthetic ultralow-molecular-weight heparin using collision-induced dissociation. *Analytical Chemistry, 84*, 5475–5478.

Kailemia, M. J., Li, L., Xu, Y., Liu, J., Linhardt, R. J., & Amster, I. J. (2013). Structurally informative tandem mass spectrometry of highly sulfated natural and chemoenzymatically synthesized heparin and heparan sulfate glycosaminoglycans. *Molecular & Cellular Proteomics, 12*, 979–990.

Kinoshita, A., & Sugahara, K. (1999). Microanalysis of glycosaminoglycan-derived oligosaccharides labeled with a fluorophore 2-aminobenzamide by high-performance liquid chromatography: application to disaccharide composition analysis and exo-sequencing of oligosaccharides. *Analytical Biochemistry, 269*, 367–378.

Lee, S., Raw, A., Yu, L., Lionberger, R., Ya, N., Verthelyi, D., et al. (2013). Scientific considerations in the review and approval of generic enoxaparin in the United States. *Nature Biotechnology, 31*, 220–226.

Li, L., Zhang, F., Zaia, J., & Linhardt, R. J. (2012). Top-down approach for the direct characterization of low molecular weight heparins using LC-FT-MS. *Analytical Chemistry, 84*, 8822–8829.

Li, D., Chi, L., Jin, L., Xu, X., Du, X., Ji, S., et al. (2014). Mapping of low molecular weight heparins using reversed phase ion pair liquid chromatography-mass spectrometry. *Carbohydrate Polymers, 99*, 339–344.

Li, G., Steppich, J., Wang, Z., Sun, Y., Xue, C., Linhardt, R. J., et al. (2014). Bottom-up low molecular weight heparin analysis using liquid chromatography-Fourier transform mass spectrometry for extensive characterization. *Analytical Chemistry, 86*, 6626–6632.

Liverani, L., Mascellani, G., & Spelta, F. (2009). Heparins: process-related physico-chemical and compositional characteristics: fingerprints and impurities. *Thrombosis and Haemostasis, 102*, 846–853.

Maxwell, E., Tan, Y., Tan, Y., Hu, H., Benson, G., Aizikov, K., et al. (2012). GlycReSoft: a software package for automated recognition of glycans from LC/MS data. *Public Library Of Science, 7*, e45474.

Mourier, P. A. J., & Viskov, C. (2004). Chromatographic analysis and sequencing approach of heparin oligosaccharides using cetyltrimethylammonium dynamically coated stationary phases. *Analytical Biochemistry, 332*, 299–313.

Mourier, P. A. J., Agut, C., Souaifi-Amara, H., Herman, F., & Viskov, C. (2015). Analytical and statistical comparability of generic enoxaparins fromthe US market with the originator product. *Journal of Pharmaceutical and Biomedical Analysis, 115*, 431–442.

Ozug, J., Wudyka, S., Gunay, N. S., Beccati, D., Lansing, J., Wang, J., et al. (2012). Structural elucidation of the tetrasaccharide pool in enoxaparin sodium. *Analytical and Bioanalytical Chemistry, 403*, 2733–2744.

Pervin, A., Al-Hakin, A., & Linhardt, R. J. (1994). Separation of glycosaminoglycan-derived oligosaccharides by capillary electrophoresis using reverse polarity. *Analytical Biochemistry, 221*, 182–188.

Skidmore, M. A., Guimond, S. E., Dumax-Vorzet, A. F., Yates, E. A., & Turnbull, J. E. (2010). Disaccharide compositional analysis of heparan sulfate and heparin polysaccharides using UV or high-sensitivity fluorescence (BODIPY) detection. *Nature Protocols, 5*, 1983–1992.

Sun, X., Lin, L., Liu, X., Zhang, F., Chi, L., Xia, Q., et al. (2016a). Capillary electrophoresis-mass spectrometry for the analysis of heparin oligosaccharides and low molecular weight heparin. *Analytical Chemistry, 88*, 1937–1943.

Sun, X., Sheng, A., Liu, X., Shi, F., Jin, L., Xie, S., et al. (2016b). Comprehensive identification and quantitation of basic building blocks for low-molecular weight heparin. *Analytical Chemistry, 88*, 7738–7744.

Sun, X., Guo, Z., Yu, M., Lin, C., Sheng, A., Wang, Z., et al. (2017). Hydrophilic interaction chromatography-multiple reaction monitoring mass spectrometry method for basic building blockanalysis of low molecular weight heparins prepared through nitrousacid depolymerization. *Journal of Chromatography A, 1479*, 121–128.

Venkataraman, G., Shriver, Z., Raman, R., & Sasisekharan, R. (1999). Sequencing complex polysaccharides. *Science, 286*, 537–542.

Wang, L., Reinhard, M., & Job, H. (1997). Heparins, low-molecular-weight heparins, and other glycosaminoglycans analyzed by agarose gel electrophoresis and azure A-silver staining. *Seminars in Thrombosis and Hemostasis, 23*, 11–16.

Wang, Z., Li, D., Sun, X., Bai, X., Jin, L., & Chi, L. (2014). Liquid chromatography- diode array detection-mass spectrometry for compositional analysis of low molecular weight heparins. *Analytical Biochemistry, 451*, 35–41.

Wang, Z., HSIEH, P., Xu, Y., Thieker, D., Chai, E. J. E., Xie, S., et al. (2017). Synthesis of 3-*O*-sulfated oligosaccharides to understand the relationship between structures and functions of heparan sulfate. *Journal of the American Chemical Society, 139*, 5249–5256.

Wolff, J. J., Chi, L., Linhardt, R. J., & Amster, I. J. (2007). Distinguishing glucuronic from iduronic acid in glycosaminoglycan tetrasaccharides by using electron detachment dissociation. *Analytical Chemistry, 79*, 2015–2022.

Xu, X., Li, D., Chi, L., Du, X., Bai, X., & Chi, L. (2015). Fragment profiling of low molecular weight heparins using reversed phase ion pair liquid chromatography-electrospray mass spectrometry. *Carbohydrate Research, 407*, 26–33.

Zanetta, J., Timmerman, P., & Leroy, Y. (1999). Determination of constituents of sulphated proteoglycans using a methanolysis procedure and gas chromatography/mass spectrometry of heptafluorobutyrate derivatives. *Glycoconjugate Journal, 16*, 617–627.

Zhang, Q., Chen, X., Zhu, Z., Zhan, X., Wu, Y., Song, L., et al. (2013). Structural analysis of low molecular weight heparin by ultraperformance size exclusion chromatography/time of flight mass spectrometry and capillary zone electrophoresis. *Analytical Chemistry, 85*, 1819–1827.